



UNIVERSITY OF LEEDS

This is a repository copy of *Unaltered  $\dot{V}O_2$  kinetics despite greater muscle oxygenation during heavy-intensity two-legged knee extension versus cycle exercise in humans*.

White Rose Research Online URL for this paper:  
<http://eprints.whiterose.ac.uk/148596/>

Version: Accepted Version

---

**Article:**

Koga, S, Okushima, D, Poole, DC et al. (3 more authors) (2019) Unaltered  $\dot{V}O_2$  kinetics despite greater muscle oxygenation during heavy-intensity two-legged knee extension versus cycle exercise in humans. *American Journal of Physiology - Regulatory, Integrative and Comparative Physiology*, 317 (1). R203-R213. ISSN 0363-6119

<https://doi.org/10.1152/ajpregu.00015.2019>

---

(c) 2019, the American Physiological Society. This is an author produced version of a paper published in the *American Journal of Physiology - Regulatory, Integrative and Comparative Physiology*. Uploaded in accordance with the publisher's self-archiving policy.

**Reuse**

Items deposited in White Rose Research Online are protected by copyright, with all rights reserved unless indicated otherwise. They may be downloaded and/or printed for private study, or other acts as permitted by national copyright laws. The publisher or other rights holders may allow further reproduction and re-use of the full text version. This is indicated by the licence information on the White Rose Research Online record for the item.

**Takedown**

If you consider content in White Rose Research Online to be in breach of UK law, please notify us by emailing [eprints@whiterose.ac.uk](mailto:eprints@whiterose.ac.uk) including the URL of the record and the reason for the withdrawal request.



[eprints@whiterose.ac.uk](mailto:eprints@whiterose.ac.uk)  
<https://eprints.whiterose.ac.uk/>

**Unaltered  $\dot{V}O_2$  kinetics despite greater muscle oxygenation during heavy-intensity two-legged knee extension versus cycle exercise in humans**

Shunsaku Koga,<sup>1</sup> Dai Okushima,<sup>1</sup> David C. Poole,<sup>2</sup> Harry B. Rossiter,<sup>3,4</sup> Narihiko Kondo,<sup>5</sup> and Thomas J. Barstow<sup>2</sup>

<sup>1</sup>Applied Physiology Laboratory, Kobe Design University, Kobe 651-2196, Japan.

<sup>2</sup>Departments of Anatomy and Physiology, and Kinesiology, Kansas State University,

Manhattan, Kansas 66506-0302, USA. <sup>3</sup>Rehabilitation Clinical Trials Center, Division of

Respiratory & Critical Care Physiology & Medicine, Los Angeles Biomedical Research

Institute at Harbor-UCLA Medical Center, Torrance, CA 90502, USA. <sup>4</sup>Faculty of

Biological Sciences, University of Leeds, Leeds, LS2 9JT, United Kingdom. <sup>5</sup>Applied

Physiology Laboratory, Kobe University, Kobe 657-0011, Japan.

Running title: Muscle deoxygenation kinetics in knee extension and cycle exercise

Address for Correspondence: Shunsaku Koga, Ph.D.

Applied Physiology Laboratory, Kobe Design University

8-1-1 Gakuennishi-machi, Nishi-ku, Kobe, 651-2196, Japan

## Abstract

Relative perfusion of active muscles is greater during knee extension ergometry (KE) than cycle ergometry (CE). This provides the opportunity to investigate the effects of increased O<sub>2</sub> delivery ( $\dot{Q}O_2$ ) on deoxygenation heterogeneity among quadriceps muscles and pulmonary  $\dot{V}O_2$  kinetics. Using time-resolved near-infrared spectroscopy, we hypothesized that compared with CE the superficial vastus lateralis (VL), superficial rectus femoris and deep VL in KE would have 1) a smaller amplitude of the exercise-induced increase in deoxy[Hb+Mb] (related to the balance between  $\dot{V}O_2$  and  $\dot{Q}O_2$ ); 2) a greater amplitude of total[Hb+Mb] (related to the diffusive O<sub>2</sub> conductance); 3) a greater homogeneity of regional muscle deoxy[Hb+Mb]; and 4) no difference in pulmonary  $\dot{V}O_2$  kinetics. Eight participants performed square-wave KE and CE exercise from 20 W to heavy work rates. Deoxy[Hb+Mb] amplitude was less for all muscle regions in KE (P<0.05: superficial, KE 17-24 vs. CE 19-40; deep, KE 19 vs. CE 26  $\mu$ M). Further, the amplitude of total[Hb+Mb] was greater for KE than CE at all muscle sites (P<0.05: superficial, KE 7-21 vs. CE 1-16; deep, KE 11 vs. CE -3  $\mu$ M). Although the amplitude and heterogeneity of deoxy[Hb+Mb] was significantly lower in KE than CE during the first minute of exercise, the pulmonary  $\dot{V}O_2$  kinetics was not different for KE and CE. These data show that the microvascular  $\dot{Q}O_2$  to  $\dot{V}O_2$  ratio, and thus tissue oxygenation,

was greater in KE than CE. This suggests that pulmonary and muscle  $\dot{V}O_2$  kinetics in young healthy humans are not limited by  $\dot{Q}O_2$  during heavy-intensity cycling.

**Key words:** near-infrared spectroscopy, oxygen delivery, muscle deoxygenation, heterogeneity

## **Introduction**

Despite evidence that the speed of pulmonary and muscle  $\dot{V}O_2$  kinetics in young healthy humans across the rest-exercise transition is not limited by  $O_2$  delivery ( $\dot{Q}O_2$ ) (17, 32, 43, 49) this issue remains contentious during moderate-intensity (38) and heavy-intensity exercise (43). This uncertainty may well reflect limitations in technological approaches that include single-site and superficial near-infrared spectroscopy (NIRS) interrogation of muscle deoxygenation (deoxy[Hb+Mb]) profiles or venous/mixed venous effluent sampling, and employ a range of exercise models and inter-subject differences in cardiopulmonary fitness or muscle oxidative capacity (33).

For large muscle mass exercise [e.g., conventional cycling (CE) or running exercise] where as much as 7.5 kg (for one leg) or more is recruited, the sympathetic nervous system opposes local vasodilation in an attempt to regulate mean arterial pressure for the

extant cardiac output (54). The consequence of this sympathetic action is that increases in blood flow are limited, constraining  $\dot{Q}O_2$  and changes thereof and setting fractional  $O_2$  extraction according to local  $\dot{V}O_2$  (i.e., the local  $\dot{Q}O_2/\dot{V}O_2$  ratio) (20). Small muscle mass exercise like knee extension (KE, 2-3 kg for one leg) (1, 7, 32, 34, 46) and handgrip (<1 kg) results in a far greater mass specific muscle blood flow, and therefore a greater  $\dot{Q}O_2$  ceiling, during contractions than observed in CE or running. Greater mass specific blood flow (KE,  $3.85 \text{ L}\cdot\text{min}^{-1}\cdot\text{kg}^{-1}$ ; CE,  $1.3 \text{ L}\cdot\text{min}^{-1}\cdot\text{kg}^{-1}$ ),  $\dot{Q}O_2$  and  $\dot{V}O_2$  (KE,  $>600 \text{ mL}\cdot\text{min}^{-1}\cdot\text{kg}^{-1}$ ; CE,  $230 \text{ mL}\cdot\text{min}^{-1}\cdot\text{kg}^{-1}$ ) (25, 47, 48) during exercise has the potential to increase the regional muscle  $\dot{Q}O_2/\dot{V}O_2$  ratio, which would raise microvascular  $O_2$  pressures and constrain the rise in deoxy[Hb+Mb]. Moreover, as microvascular and capillary hematocrit at rest is far below systemic (e.g., 15 vs. 45 %), and increases with elevated muscle blood flow and capillary red blood cell flux (23, 24), there is the opportunity for a greater increase in [Hb] during KE than CE (measured by quantitative NIRS as total[Hb+Mb]); such a dichotomy is expected to elevate blood-myocyte diffusive  $O_2$  transport more in KE than CE (9, 13, 42).

Recent improvements in NIRS technology including time-resolved spectroscopy (TRS-NIRS), multi-site sampling, improved penetration depth and correction for overlying adipose tissue have increased our ability to resolve spatial and temporal

exercise-induced changes in deoxy- and total[Hb+Mb] (2, 26, 28, 29, 31, 33). Moreover, TRS-NIRS abolishes the need to make assumptions regarding photon scattering and pathlength that are used in some other NIRS methodologies, and therefore provides absolute measurement of deoxy- and total[Hb+Mb]. Use of this technology has revealed substantial heterogeneities with respect to the amplitudes and kinetics of deoxygenation and [Hb] within and across muscles during CE (2, 4, 6, 16, 21, 33, 40, 41).

Our previous investigation comparing KE and CE (32) relied upon bulk  $\dot{Q}$  (whole leg blood flow) and  $\dot{V}O_2$  (pulmonary) and was unable to resolve the degree of intramuscular  $\dot{Q}O_2$ -to- $\dot{V}O_2$  matching within and among different quadriceps muscles. Since then it has become apparent that bulk  $\dot{Q}$  dynamics are very different from those extant at the microvascular level (14, 19) providing an impetus to utilize the latest in NIRS technology to investigate among different muscle depths and regions how a greater bulk  $\dot{Q}$  during KE might translate to  $\dot{Q}O_2$ -to- $\dot{V}O_2$  heterogeneity across the quadriceps.

The global hypothesis tested was that a greater bulk muscle  $\dot{Q}O_2/\dot{V}O_2$  ratio, as seen during heavy-intensity KE compared with CE, would increase the regional muscle  $\dot{Q}O_2/\dot{V}O_2$  ratio and consequently: 1) reduce the amplitude of the exercise-induced deoxy[Hb+Mb] response in KE compared with CE; 2) increase the amplitude of total[Hb+Mb] in KE compared with CE; 3) increase the homogeneity of regional muscle

deoxy[Hb+Mb] responses in KE compared with CE; but 4) not speed pulmonary  $\dot{V}O_2$  kinetics in KE compared with CE. The finding of evidence supporting hypothesis 4 would be consistent with the notion that  $\dot{V}O_2$  kinetics are not limited by  $O_2$  delivery during heavy-intensity cycling. These specific hypotheses were tested across four muscle sites: distal superficial vastus lateralis; distal superficial rectus femoris; proximal superficial rectus femoris; and proximal deep vastus lateralis.

## **Methods**

### Participants

Eight men (age,  $21 \pm 3$  years; height,  $175 \pm 3$  cm; and weight,  $65 \pm 7$  kg;  $\dot{V}O_{2peak}$  for CE =  $3.03 \pm 0.43$  L·min<sup>-1</sup>) participated in the study. All volunteers were nonsmokers and free of known respiratory, cardiovascular, and metabolic diseases, and were involved in regular exercise (ranging from recreational activity to amateur competitive sport). After a detailed explanation of the study, written informed consent was obtained. The study was approved by the Human Subjects Committee of Kobe Design University.

### Experimental Design

CE tests were performed in the upright position on an electronically braked cycle (75XL-III, Combi, Tokyo, Japan). On separate days upright two-legged KE tests were performed

on a knee extension/flexion ergometer previously described (32). The two-legged KE paradigm had advantages over one-legged KE due to a reduction of O<sub>2</sub> cost for postural support and a larger increase in amplitude of pulmonary  $\dot{V}O_2$ , which helped to quantify the precise temporal profiles of the responses. The resistance for the two-legged KE was provided via two long metal bars attached to the cranks of an electronically braked cycle ergometer positioned behind the seated subject. Each foot was placed in an Achilles-bracing heel-cup. The alternate movement of both legs required smoothly coordinated and continuous movement in a very similar manner to that of standard cycle ergometer exercise (11). The KE was performed through 40° of knee extension and flexion (90–130°) in an alternating kicking pattern, i.e., while one leg was extending, the other was flexing. The ergometer had an adjustable backrest that allowed the participants to sit with a hip angle of ~100°. The previous studies reported the flexion phase of the KE movement was "passive" (1, 46, 51). Thus, the participants were instructed not to contract the muscles during the flexion phase for rotating the crank of cycle ergometer and thereafter had several familiarization sessions before conducting the exercise test. In contrast during CE, there were active flexion/pull-back with increase in the EMG amplitudes of vastus lateralis (VL) and rectus femoris (RF) (27). This would influence the amount of active muscle mass for KE and CE, however, the mass-specific metabolic demands of small

muscle mass KE are greater than CE, i.e., a larger  $\dot{V}O_2$  gain per muscle mass in KE (32).

For each exercise session participants reported to the laboratory at least 2 h after their last meal. They were asked to avoid caffeine, alcohol, and strenuous exercise for 24 h before the test. All experiments were conducted in environmental chamber (FLC-2700S; Fuji Medical Science, Chiba, Japan) and the ambient temperature and relative humidity of the chamber were maintained at 22 °C and 50 %, respectively.

#### Incremental Exercise Tests

Ramp incremental exercise protocols, preceded by 2-min rest and 4-min baseline exercise (20 W) on KE and CE ergometers, were performed to estimate each individual's gas exchange threshold (GET) and peak pulmonary  $O_2$  uptake ( $\dot{V}O_{2peak}$ ) for each exercise mode. The work rate for the ramp incremental exercise were  $10 \text{ W}\cdot\text{min}^{-1}$  for KE and  $20 \text{ W}\cdot\text{min}^{-1}$  for CE tests. Participants were instructed to maintain kicking frequency at 60 contractions per minute per leg for KE and pedal frequency at 60 rpm for CE. KE and CE conditions were randomized and tested on separate days.

#### Constant Power Exercise Tests

On separate days, constant power exercise tests were performed for 6 min, preceded by 2-min rest and 4-min baseline exercise (20 W). Heavy-intensity power output for KE ( $82 \pm 10 \text{ W}$ ) and CE ( $189 \pm 22 \text{ W}$ ) were based on the power equivalent of 40 % of the

difference between the GET and  $\dot{V}O_{2\text{peak}}$  ( $\Delta 40\%$ ), based on the initial ramp incremental exercise in each exercise condition. Participants performed two to three exercise transitions for KE and two exercise transitions for CE over a four-week period. Only one heavy exercise transition was performed on each day.

## Measurements

### *Pulmonary oxygen uptake ( $\dot{V}O_2$ )*

Participants breathed through a low-resistance hot-wire flowmeter for measurement of inspiratory and expiratory flows (model AE-300S; Minato-Medical, Osaka, Japan). The flowmeter was calibrated repeatedly by inputting known volumes of room air at various mean flows and flow profiles. Expired  $O_2$  and  $CO_2$  concentrations were determined by gas analysis (model AE-300S; Minato-Medical, Osaka, Japan) from a sample drawn continuously from the mouthpiece. Precision-analyzed gas mixtures were used for calibration. Alveolar gas exchange variables were calculated breath-by-breath according to the algorithms of Beaver et al. (3). Heart rate was monitored continuously via a three-lead ECG.

### Time-resolved near-infrared spectroscopy (TRS-NIRS)

The principles of operation and algorithms utilized by the equipment have been described in detail elsewhere (29, 31, 39). Briefly, a high-frequency light pulser emits

light at three wavelengths, and a single-photon detector measures the light reflected from the material or tissues under the probe at 5 MHz. This detection-time curve is fitted to resolve the absorption coefficient, the reduced scattering coefficient, and the mean pathlength, by application of diffusion theory. Knowledge of these three variables allows measurement of absolute deoxy[Hb+Mb] and oxy[Hb+Mb] in  $\mu\text{M}$  units, and their sum, total[Hb+Mb]. From these, tissue  $\text{O}_2$  saturation ( $S_t\text{O}_2$ ) is calculated by  $\text{oxy[Hb+Mb]}/\text{total[Hb+Mb]}*100$ . The TRS-NIRS technology is based on fitting of the light diffusion curve (the photon distribution of the time-of-flight) and known speed of light. The diffusion curve parameters are independent of the tissue through which the light is traveling—the values of the parameters are measured. Therefore, the technology itself does not depend on the structure or volume distribution of the microvasculature or [Mb] within the tissue investigated.

The absolute changes in muscle deoxygenation and oxygenation profiles during KE and CE were measured in the quadriceps of the dominant leg. Two TRS-NIRS (TRS-20; Hamamatsu Photonics K.K., Hamamatsu, Japan) were used to measure deoxygenation in the superficial regions of VL (distal site, dVL-s) and RF muscles (distal and proximal sites, dRF-s and pRF-s), and a high-power TRS-NIRS (TRS-20SD; Hamamatsu Photonics K.K., Hamamatsu, Japan) was used to measure deoxygenation (21, 26, 29, 41)

in the deep VL (proximal site, pVL-d). The output frequency of both TRS systems was set to 0.5 Hz. Calibration of both instruments was performed before each test by measuring the response when the input and receiving fibers face each other through a neutral-density filter in a black tube.

The skin under the probes was carefully shaved and optodes, housed in black rubber holders that helped to minimize extraneous movement, were fixed to the skin with adhesive tape. For superficial muscles, the interoptode spacing (OS) between irradiation and detection probes was 3 cm. The optodes were placed on the distal sites of the VL and RF, and proximal site of RF muscle parallel to the major axis of the thigh. For deep muscle, the OS of 6 cm was used and the optodes were placed on the proximal site of the VL muscle.

At the end of the exercise test pen marks were made on the skin to indicate the margins of the rubber NIRS optode holders so that adipose tissue thickness (ATT) could be subsequently measured. The ATT thicknesses were measured at rest with the subject in an upright-seated position using B-mode ultrasound (Logiq 400; GE-Yokogawa Medical Systems, Tokyo, Japan). ATT was measured at the TRS-NIRS optode site of the VL and RF muscles. In order to quantify the influence of ATT on dynamic changes in NIRS signals, we used the ATT correction method of Bowen et al. (4), using a linear regression

of the relationship between total[Hb+Mb] and ATT at rest ( $\text{total[Hb+Mb]} = -17.0 * [\text{ATT}] + 203$ ,  $r^2 = 0.754$ ,  $P < 0.001$ ). This normalization process allowed absolute values of both deoxy- and total[Hb+Mb] to be compared among subjects and muscle sites differing in ATT (e.g., 29).

### Surface electromyography

Surface electromyography (EMG) was measured in order to estimate muscle activation near the TRS-NIRS optode sites of the VL and RF muscles. Three separate bipolar EMG sensors were connected to a multi-channel data acquisition system (MP100; Biopac systems, Goleta, USA) through an amplifier (Polyam 4; NIHON SANTEKU Co., Osaka, Japan), with a sampling frequency of 1 kHz. Electrodes (Bluesensor T-00-S; Ambu, Ballerup, Denmark) were positioned just proximal to the NIRS optode assembly on the VL and RF, and all sites were prepared by shaving, abrading, and cleaning the skin with alcohol and preconditioning agent (Skin pure; NIHON KODEN, Tokyo, Japan). Before data collection the EMG sensor body was secured to the leg with surgical tape to help minimize any sensor movement and reduce noise during exercise.

Further, subjects performed three repetitions of maximal voluntary contractions (MVC) while seated upright on a chair. The MVC was measured during 7-s maximal contractions by having subjects extend their dominant leg against an immovable bar. Subjects were

allowed to rest for at least 3 min before performing the each MVC. The integrated EMG (iEMG) of the individual muscles was normalized to the MVC (the peak instantaneous EMG during the highest EMG of the three efforts), as expressed % MVC.

### Kinetic Analysis

After aberrant values of pulmonary  $\dot{V}O_2$  and deoxy[Hb+Mb] greater than three SD's from the local mean were omitted, the individual responses during the baseline-to-exercise transitions were time-interpolated to 1 s intervals, and averaged across each transition for each subject. The response curve of  $\dot{V}O_2$  was fitted to a three-term exponential function (Eq. 1) that included amplitudes, time constants, and time delays, using nonlinear least-squares regression techniques (Kaleida Graph ver. 4.5; Synergy Software, Reading, USA) (e.g., 16, 31). The first exponential term started with the onset of exercise and the second and third terms began after independent time delays (35).

$$H(t) = 0 \text{ for } t < 0$$

$$1 \text{ for } t \geq 0$$

$$\begin{aligned} \dot{V}O_2(t) = \dot{V}O_2(\text{BL}) + H \cdot (t) \cdot A_c \cdot (1 - e^{-t/\tau_c}) & \quad \text{phase I (cardiodynamic component) (1)} \\ + H \cdot (t - \text{TD}_p) \cdot A_p \cdot [1 - e^{-(t - \text{TD}_p)/\tau_p}] & \quad \text{phase II (primary component)} \\ + H \cdot (t - \text{TD}_s) \cdot A_s \cdot [1 - e^{-(t - \text{TD}_s)/\tau_s}] & \quad \text{phase III (slow component, SC)} \end{aligned}$$

where the subscripts c, p, and s refer to initial, primary, and slow components,

respectively;  $\dot{V}O_2$  (BL) is the baseline value (20 W exercise);  $A_c$ ,  $A_p$ , and  $A_s$  are the asymptotic amplitudes for the exponential terms;  $\tau_c$ ,  $\tau_p$ , and  $\tau_s$  are the time constants; and  $TD_p$ , and  $TD_s$  are the time delays. The phase I  $\dot{V}O_2$  at the start of phase II (i.e., at  $TD_p$ ) was assigned the value of  $\dot{V}O_2$  at  $t = TD_p$  ( $A_c'$ ). The physiologically relevant amplitude of the primary exponential component during phase II ( $A_p'$ ) was defined as the sum of  $A_c' + A_p$ . To facilitate comparison among participants at different absolute work rates, the  $O_2$  cost (gain) of the primary response was calculated as  $G_p$  ( $A_p'/\Delta\text{power}$ ), where  $\Delta\text{power}$  is the increase in power output above the 20 W baseline.

Because of concerns regarding the validity of using the extrapolated asymptotic value for the slow component ( $A_s$ ), we used the value of fitted function at  $t = 6$  min (end exercise;  $A_s'$ ) to define the relative contribution of slow component to the overall increase in  $\dot{V}O_2$  [ $A_s'/(A_p' + A_s')$ ]. The increment in  $\dot{V}O_2$  between the 3rd and 6th min of exercise ( $\Delta\dot{V}O_{2\ 6-3}$ ) was also calculated as an index of the  $\dot{V}O_2$  slow component amplitude.

The deoxy[Hb+Mb] data were fit with a monoexponential model (Eq.2):

$$\text{deoxy[Hb+Mb]}_{(t)} = \text{deoxy[Hb+Mb]}_b + A_p \cdot [1 - e^{-(t-TD_p)/\tau_p}] \quad (2)$$

where the subscripts b and p refer to baseline 20 W cycling and primary component, respectively;  $\text{deoxy[Hb+Mb]}_b$  is the 20 W exercise baseline value;  $A_p$  is the amplitude of the exponential term;  $\tau_p$  is the time constant and  $TD_p$  represents the initial component

time delay. The deoxy[Hb + Mb] data were fit from the time of exercise onset to 180 s with the mono-exponential model (29). In our previous study (30), we compared the  $TD_p$  values of a single-exponential model (14, 18, 22) with those of a two-exponential model (30) and DeLorey et al. (10; the  $TD_p$  from the time of exercise onset to the first point greater than 1 SD above the mean of the baseline). At some sites, there were no significant differences in the  $TD_p$  for the three methods, while at others sites our method produced slightly shorter  $TD_p$  values (1–2 s).

The  $TD_p$  and  $\tau_p$  of the deoxy[Hb+Mb] response were summed to provide an indication of the overall dynamics of muscle deoxygenation in the first 3 min of exercise (mean response time, MRT). Separately, values for deoxy[Hb+Mb], oxy[Hb+Mb], and total[Hb+Mb] were measured from the mean of the last 60 s at baseline, and the 30 s immediately before 3 and 6 min of exercise.

The increment in deoxy[Hb+Mb] between the 3rd and 6th min of exercise ( $\Delta$  Amplitude<sub>6-3</sub>) was also calculated as an index of the slow component amplitude. Further, the relative contribution of slow component to the overall increase ( $\Delta$ Amplitude<sub>6-3</sub>/Amplitude at 6 min) was also calculated.

As a measure of “data point-by-data point” inter-site heterogeneity of the deoxy- and total[Hb+Mb], root mean squared error (RMSE) for each subject at a given time was

calculated as follows (50):

$$\text{RMSE}(t) = \sqrt{\left[ \sum (X_i - X_{\text{ave}})^2 / n \right]}$$

where  $X_i$ ,  $X_{\text{ave}}$ , and  $n$  are individual responses at each site, the mean of the 4 sites values, and the number of the sites (i.e., 4), respectively.

Further, amplitudes of deoxy- and total[Hb+Mb] normalized to iEMG (i.e.,  $\mu\text{M} \cdot \% \text{MVC}^{-1}$ ) were calculated from the mean of the 30 s immediately before 3 min of exercise.

## Statistics

Data are presented as mean  $\pm$  SD. Paired-samples t-tests were used to compare the  $\dot{V}\text{O}_2$  kinetic parameters between the KE and CE. The differences in NIRS parameter and iEMG (% MVC) values were analyzed by using repeated measures analysis of variance across exercise mode (KE vs. CE) and muscle site (dVL-s, dRF-s, pRF-s and pVL-d) with Tukey's adjusted post-hoc tests. Statistical significance was accepted when  $P < 0.05$ . A statistical software (GraphPad Prism ver. 7.02, GraphPad Software, San Diego, USA) was used for each test. Effect sizes (ES: using Cohen's  $d$  and  $\eta^2_p$ ) and statistical power ( $1-\beta$ ) were calculated for the pulmonary  $\dot{V}\text{O}_2$  and NIRS variables.

## Results

Adipose tissue thickness (ATT)

The ATT of the distal sites of VL and RF, and proximal site of VL and RF were  $4.1 \pm 1.0$ ,  $5.6 \pm 1.5$ ,  $7.0 \pm 2.9$ , and  $5.7 \pm 2.1$  mm, respectively. There were no significant ATT differences among sites.

#### Pulmonary $\dot{V}O_2$ responses

As expected, GET and  $\dot{V}O_{2peak}$  were significantly lower for KE than CE (GET:  $1.13 \pm 0.17$  vs.  $1.38 \pm 0.17$  L·min<sup>-1</sup>,  $P < 0.01$ ,  $d = 1.46$ ,  $1-\beta = 0.94$ ;  $\dot{V}O_{2peak}$ :  $1.81 \pm 0.41$  vs.  $3.03 \pm 0.43$  L·min<sup>-1</sup>,  $P < 0.01$ ,  $d = 2.90$ ,  $1-\beta = 0.99$ ). Fig. 1a shows pulmonary  $\dot{V}O_2$  responses to KE and CE heavy-intensity exercise, and mean kinetic parameters are given in Table 1. Both CE and KE responses exhibited a slow component, as is characteristic of heavy-intensity exercise. However, the relative amplitude of the  $\dot{V}O_2$  slow component [i.e.,  $A'_s/(A'_p+A'_s)$ ] was not different for the two exercise modes. The  $O_2$  cost of the primary component  $\dot{V}O_2(G_p)$  was greater in KE than CE ( $P < 0.05$ ,  $d = 1.69$ ,  $1-\beta = 0.98$ ) (Fig. 1b) and, importantly, the pulmonary  $\dot{V}O_2$  time constant was not different for KE and CE.

#### Muscle deoxy- and total[Hb+Mb] responses among the superficial regions

The temporal profiles of deoxy[Hb+Mb] during KE and CE are shown in Fig. 2. Exercise-induced deoxy[Hb+Mb] increase (amplitude) in the d-VLs muscle was considerably greater in CE than KE ( $40 \pm 27$  vs.  $25 \pm 14$   $\mu\text{M}$ ;  $P < 0.05$ ,  $d = 0.70$ ,  $1-\beta =$

0.40) (Table 2). Overall, the amplitude of deoxy[Hb+Mb] at both 3 and 6 min was significantly lower for KE than CE in all muscle regions except at dRF-s (Table 3).

The primary component kinetics of deoxy[Hb+Mb] were significantly different between KE and CE (Table 2 and Figs. 2 and 3). For CE, the MRT was shortest in the dVL-s ( $19 \pm 4$  s) and longest in the pRF-s ( $51 \pm 23$  s) (Table 2). The opposite was observed for KE, with the MRT for dVL-s being the longest ( $51 \pm 16$  s) and shortest for pRF-s ( $25 \pm 12$  s). Neither the slow component of deoxy[Hb+Mb] ( $\Delta\text{Amplitude}_{6-3}$ ) nor its relative contribution were different between KE and CE at any muscle site (Table 3).

The exercise-induced increase in total[Hb+Mb] was greater for KE than CE (Table 4 and Fig. 4). In particular, the amplitude of total[Hb+Mb] at 3 min was significantly greater for KE than CE at each muscle site ( $P < 0.05$ ,  $\eta^2_p = 0.49$ ,  $1-\beta = 0.96$ ) (Table 4).

Muscle deoxy- and total[Hb+Mb] responses in the proximal deep VL muscle

A low S/N ratio precluded confident kinetic modeling of the deoxy[Hb+Mb] response in pVL-d, and hence these data are omitted from Table 2. The overall deoxy[Hb+Mb] amplitude of the pVL-d was less for KE than CE ( $P < 0.05$ ,  $d = 1.37$ ,  $1-\beta = 0.91$ ; Fig. 2 and Table 3). Fig. 3 compares pulmonary  $\dot{V}O_2$  kinetics with the kinetics of muscle deoxygenation in the superficial and deep VL for both exercise modes.

The amplitude of total[Hb+Mb] in the pVL-d was significantly greater for KE than CE

( $P < 0.05$ ,  $d = 1.37$ ,  $1-\beta = 0.98$ ; Fig. 4 and Table 4).

Fig. 5 shows the point-by-point RMSE for all participants, illustrating the heterogeneity of deoxy- and total[Hb+Mb] responses to exercise across the quadriceps muscles for KE and CE. Heterogeneity of deoxy[Hb+Mb] was significantly lower in KE than CE during the 1st min of exercise (Panel a;  $P < 0.05$ ,  $\eta^2_p = 0.23$ ,  $1-\beta = 1.00$ ). However, heterogeneity of the total[Hb+Mb] response was not different between KE and CE (Panel b;  $\eta^2_p = 0.15$ ,  $1-\beta = 0.99$ ).

Muscle deoxy- and total[Hb+Mb] responses normalized to muscle activity profiles

Group mean responses of muscle activity (iEMG) relative to MVC (% MVC) during the last 30 s immediately before the end of exercise are shown in Fig. 6 ( $n = 7$ ). For CE, the VL was activated at a substantially higher proportion of its MVC than the distal RF. In contrast, relative muscle activity across all muscle sites did not differ for KE.

Further, when the deoxy[Hb+Mb] amplitudes were normalized to iEMG, the KE versus CE differences were abolished (Fig. 7a). In addition, the amplitudes of total[Hb+Mb] normalized to muscle activity were greater for KE than CE for all sites ( $P < 0.05$ ,  $\eta^2_p = 0.39$ ,  $1-\beta = 0.46$ ) (Fig. 7b).

## Discussion

Our primary original findings provided evidence for enhanced perfusive and diffusive O<sub>2</sub> transport within the quadriceps musculature for KE compared with CE. Thus, if O<sub>2</sub> delivery per se were limiting the speed of the  $\dot{V}O_2$  kinetics during CE, pulmonary  $\dot{V}O_2$  kinetics should be faster during KE than CE. However, pulmonary  $\dot{V}O_2$  kinetics (time constant) were not different between the two exercise modes.

#### Pulmonary $\dot{V}O_2$ responses

There were no significant differences in the time delay or time constant of pulmonary  $\dot{V}O_2$  primary component kinetics between CE and KE (Table 1) [consistent with Cleland et al. (7) and Koga et al. (32)].

The slower pulmonary  $\dot{V}O_2$  kinetics during KE versus CE reported by Shoemaker et al. (52) may have resulted from the same absolute work rate constituting a greater relative intensity (and domain) as well as sustained muscle tension during KE restricting blood flow (lifting and lowering a weight) (11, 15). Herein, we ensured that all exercise was performed in the heavy-intensity domain and also that the rhythmic cycling action was not appreciably different between KE and CE. Further, MacDonald et al. (36) showed that slower increases in pulmonary  $\dot{V}O_2$  at the onset of KE in the supine compared with upright position. However, that the leg blood flow increased faster than  $\dot{V}O_2$  in the upright

position suggests under normal conditions (e.g., upright cycling),  $O_2$  utilization may limit the  $\dot{V}O_2$  response, whereas conditions such as supine body position, hypoxia, and other perturbations may produce a maldistribution of  $\dot{Q}O_2$  to  $O_2$  requirement within the exercising muscle reducing local  $O_2$  delivery into the “ $O_2$  delivery-dependent range.” (32, 43).

The relative amplitude of the  $\dot{V}O_2$  slow component [i.e.,  $A'_s/(A'_p+A'_s)$ ] was not different for the two exercise modes [consistent with Cleland et al. (7)]. The presence of a slow component during heavy exercise is likely to be associated with 1) recruitment of lower efficiency fibers that have a higher  $O_2$  cost per unit tension development and a longer time constant (e.g., 34, 43) and 2) an inadequate microvascular  $O_2$  delivery to the working muscles (32). In our previous study (32), we speculated that the greater normalized  $\dot{V}O_2$  slow component in KE may have resulted from increased  $\dot{Q}O_2$ -to- $\dot{V}O_2$  heterogeneity due to greater muscle tension. Fig. 2 demonstrates this not to be the case with respect to deoxy[Hb+Mb] and Figs. 4, 5 and 6 corroborate this conclusion from the perspectives of total[Hb+Mb] RMSE analysis and iEMG, which show more homogeneous profiles across muscles for KE than CE. The greater normalized  $\dot{V}O_2$  slow component in KE compared with CE reported in Koga et al. (32) suggests a compromised the matching of  $O_2$  delivery to  $O_2$  requirement, which may have resulted from e.g. a greater metabolic demand of that

muscle region or a higher intramuscular tension limiting O<sub>2</sub> delivery. Further study is required to clarify reasons for the discrepancies of the  $\dot{V}O_2$  slow component data between our previous and present studies.

### Muscle deoxygenation responses

Compared with CE, the overall amplitude of the muscle deoxy[Hb+Mb] at 6 min for KE was reduced at all muscle sites investigated in both the RF and VL, reflecting a higher  $\dot{Q}O_2/\dot{V}O_2$  ratio across the quadriceps for KE.

The kinetics ( $\tau$  and MRT) for the primary component of deoxy[Hb+Mb] at the dVL-s were significantly slower for KE compared with CE, suggesting that following the onset of exercise at the dVL-s site the  $\dot{Q}O_2/\dot{V}O_2$  ratio was higher and thus microvascular O<sub>2</sub> delivery was better matched to utilization for KE compared with CE (Fig. 2). In contrast, the faster primary component deoxy[Hb+Mb] kinetics at the pRF-s for KE may reflect a transient paucity of microvascular O<sub>2</sub> delivery relative to O<sub>2</sub> requirement. One possible explanation for the faster deoxygenation kinetics at the pRF-s of KE compared with CE is that a higher intramuscular tension in KE at the proximal RF may have impeded muscle microvascular blood flow. If true, this could have compromised the matching of microvascular  $\dot{Q}O_2$  to  $\dot{V}O_2$ . In turn, this could have masked any potential increase in

perfusion that may have resulted from recruitment of a smaller muscle mass in KE (e.g., over-perfusion to non-recruited muscle fibers) (32, 37). Therefore, the reason(s) for the faster deoxygenation kinetics at the proximal RF during KE compared with CE is currently unknown.

Based upon the muscle deoxygenation profiles, our previous study (32) suggested that bulk O<sub>2</sub> delivery to the relatively smaller exercising muscle mass at the onset of heavy KE was adequate. If there is indeed an O<sub>2</sub> delivery limitation to pulmonary  $\dot{V}O_2$  kinetics during CE, then the enhanced perfusive and diffusive O<sub>2</sub> transport within the quadriceps would be expected to speed pulmonary  $\dot{V}O_2$  kinetics during KE. However, the primary component kinetics of pulmonary  $\dot{V}O_2$  (time constant) was unaltered, which is consistent with the absence of O<sub>2</sub> delivery-limited pulmonary  $\dot{V}O_2$  kinetics during heavy-intensity exercise.

It is likely that, compared with CE, the lower RMSE of the deoxy[Hb+Mb] for KE across the exercise on-transient (Fig. 5) is partially due to the spatially homogeneous profiles of muscle activation among the muscles for KE (Fig. 6). Thus, the more homogeneous profiles of deoxy[Hb+Mb] kinetics suggest better matching of  $\dot{Q}O_2$  to  $\dot{V}O_2$  across the quadriceps musculature as a whole for KE compared with CE; in particular, for the superficial VL muscle, there may exist an admixture consisting of a greater proportion of

microvascular units adjacent to active (high  $\dot{V}O_2$ ) muscle fibers and with high microvascular  $PO_2$ , combined with a smaller portion of units that perfuse less- or non-recruited muscle fibers i.e., differences in the recruitment pattern of microvascular units based on different regional metabolic rates during KE compared with CE. Vogiatzis et al. (53) showed that in fit young subjects there is very little heterogeneity in  $\dot{Q}O_2/\dot{V}O_2$  during CE in the quadriceps, suggesting that within muscles  $\dot{Q}O_2$  is tightly matched to  $\dot{V}O_2$ . In contrast, the present and previous observations from our laboratory (e.g., 26, 29) demonstrate considerable heterogeneity of  $\dot{Q}O_2$  and  $\dot{V}O_2$  during CE especially when metabolic conditions are changing profoundly as exemplified by the exercise on-transient.

To examine the role of  $\dot{Q}O_2$  as a limiting factor for the adjustment of  $\dot{V}O_2$ , caution is required to compare the deoxy- and total[Hb+Mb] data from two different exercise modalities, performed at different absolute metabolic rates. In this context, when the deoxy[Hb+Mb] amplitudes were normalized to iEMG (% MVC), the KE versus CE differences were abolished (Fig. 7). The similarity in the microvascular  $O_2$  extraction [corrected by the iEMG (% MVC)] for KE and CE suggests that, at equivalent muscle activation levels, the muscle deoxygenation responses are independent of the exercise modes across different muscle sites [analog to bulk leg  $O_2$  extraction for the two exercise modes (48)]. It is likely that the increased blood flow is well matched to the greater mass-

specific metabolic demand for KE, which results in the lack of a difference in microvascular  $O_2$  extraction for across exercise modes.

The absolute baseline deoxy[Hb+Mb] was higher in KE than CE. As the absolute power output and the whole-body  $\dot{V}O_2$  at baseline level were identical in KE and CE, the mass-specific metabolic demands of small muscle mass KE (4 kg muscle for two legs) were expected to be far greater than CE (15 kg muscle for two legs). This suggests greater intramuscular  $\dot{V}O_2$  was required during KE than CE at baseline, and thus the exercise was initiated from a greater intramuscular  $\dot{V}O_2/\dot{Q}O_2$  in KE (i.e., the metabolic demand exceeds the  $O_2$  delivery), despite an expected higher perfusion in KE compared with CE. Interestingly, the total[Hb+Mb] concentration at baseline was also identical in KE and CE. Considering that capillary hematocrit increases with elevated perfusion as exercise intensity increases some elevation of total[Hb+Mb] was expected with the increased metabolic demand (8, 44). That the present observations did not fulfill this expectation raises interesting questions regarding microvascular control in human muscles in vivo. Currently the precise mechanism(s) for the higher deoxy[Hb+Mb] at the baseline in KE than CE are unclear.

The slow component of deoxy[Hb+Mb] ( $\Delta$ Amplitude<sub>6-3</sub>) and the relative contribution of the slow component to the overall deoxy[Hb+Mb] increase were not different between

KE and CE at any muscle site. These results suggest that, compared with CE, the enhanced perfusive and diffusive  $O_2$  transport within the quadriceps for KE may not have improved the local balance between muscle  $\dot{Q}O_2$  and  $O_2$  utilization whilst the slow component was developing.

It is crucial that the metabolic demands of different muscles be accounted for in order to discern between a fundamental alteration of the  $\dot{Q}O_2/\dot{V}O_2$  ratio versus differences resulting from altered recruitment/ $\dot{V}O_2$  relationships per se (regardless of whether it is in the same or a different muscle). While comparison of the responses to KE versus CE in this study offers a novel window into this issue, the following remain to be determined:

1) To what degree is a higher  $\dot{Q}O_2$  to  $\dot{V}O_2$  ratio (and microvascular  $PO_2$ ) beneficial in terms of optimizing muscle  $\dot{V}O_2$  kinetics and metabolic control in a specific region? 2)

When might another spatially distinct muscle region derive more benefit from some of the 'extra'  $O_2$  delivery (33)? 3) In order to interpret the dynamic adjustment of  $O_2$  delivery based on a given profile of  $O_2$  extraction (i.e., deoxy[Hb+Mb]) at each site of NIRS inspection, a  $\dot{V}O_2$  value for each of those sites should be known. Further investigation is needed to establish how differences in muscle activation might contribute to the kinetics differences we observed in CE versus KE.

Total[Hb+Mb] responses

In addition to the enhanced perfusive O<sub>2</sub> delivery discussed above, the potential for differences in muscle O<sub>2</sub> diffusing capacity (D<sub>m</sub>O<sub>2</sub>) between KE and CE must be considered. Specifically, as D<sub>m</sub>O<sub>2</sub> is determined by the volume of red blood cells in the capillary bed adjacent to muscle fibers at any instant (13, 16), the greater increase in total[Hb+Mb] with KE compared with CE exercise (Figs. 4 and 7) predicts a greater diffusive O<sub>2</sub> conductance.

We evaluated a macroscopic heterogeneity of O<sub>2</sub> delivery and  $\dot{V}O_2$  during exercise, which is impacted by differences in motor unit/muscle recruitment patterns. However, further studies must exploit technology that can address microscopic as well as macroscopic heterogeneity in vascular and metabolic control that would encapsulate the broad extremities of the O<sub>2</sub> delivery and  $\dot{V}O_2$  ratios within and among contracting muscle(s) (16).

Although KE is a unique exercise mode in that only the quadriceps are exposed to increased metabolic demand, in daily life activity there is great interest in utilizing KE for training/rehabilitation programs (e.g., repeated chair sit-to-stand exercise is prognostic in ageing and chronic lung and heart disease) where, for example, chronic obstructive

pulmonary disease or heart failure patients have an abnormally low exercise capacity consequent to limited pulmonary or cardiovascular function. Exercise training using KE has significantly and substantially increased whole-body exercise capacity and reduced exercise intolerance in heart failure (reduced ejection fraction) patients. Indeed, the KE training was so effective that it returned whole-body  $\dot{V}O_2$  to healthy control values (5, 12, 45).

#### Experimental limitations

A limitation of this study is that it is conducted with a relatively homogeneous cohort of Japanese college-aged recreationally-trained men. A larger number of subjects is required, across a wider range of physical function, (e.g., young vs. old; men vs. women) to increase the generalizability of our findings.

In conclusion, using powerful TRS-NIRS technology this investigation has, for the first time, compared the exercise modes of KE and CE to gain insights into the influence of deoxygenation heterogeneity across the quadriceps muscles on  $\dot{V}O_2$  kinetics. Specifically, despite the far greater mass-specific metabolic demands of KE, and consistent with hypothesis 1, the amplitudes of deoxy[Hb+Mb] during exercise were lower, indicative of a higher perfusive  $O_2$  conductance relative to  $\dot{V}O_2$  (i.e.,  $\dot{Q}O_2/\dot{V}O_2$  ratio) across multiple

quadriceps sites. During the exercise on-transients for both KE and CE exercise the primary component deoxy[Hb+Mb] kinetics were heterogeneous, but more so for CE than KE, evidencing a range of microvascular  $\dot{Q}O_2/\dot{V}O_2$  ratio dynamics in select quadriceps muscles, in agreement with hypothesis 3. Further, the greater amplitude of total[Hb+Mb] for KE among quadriceps muscles suggests that KE increased the diffusive  $O_2$  conductance more than CE (hypothesis 2). Collectively, these data demonstrate unaltered  $\dot{V}O_2$  kinetics for KE despite the presence of greater perfusive and diffusive  $O_2$  conductances across multiple sites within the quadriceps providing novel additional support for the concept that  $O_2$  delivery per se did not limit  $\dot{V}O_2$  kinetics during either heavy-intensity KE or CE (hypothesis 4). This underscores that pulmonary and muscle  $\dot{V}O_2$  kinetics for both KE and CE most likely reflect intramuscular limitations rather than  $O_2$  delivery limitations (e.g., 49, 55).

### Perspectives and Significance

This study demonstrates that  $\dot{V}O_2$  kinetics was not different for KE versus CE despite greater perfusive and diffusive  $O_2$  conductances across multiple sites within the quadriceps compared with CE, providing additional support for the concept that  $O_2$  delivery per se does not limit  $\dot{V}O_2$  kinetics during either heavy-intensity KE or CE. Future

studies will aim to identify whether the same is true during healthy aging or in chronic disease states. The present investigation lays valuable groundwork for construction and testing of hypotheses in patient populations where altered  $\dot{Q}O_2$ -to- $\dot{V}O_2$  heterogeneity may be linked to exercise intolerance. Further, the present observations suggest that caution is required when extrapolating the muscle  $\dot{V}O_2$  kinetics for heavy-intensity CE from KE, because the microvascular as well as the bulk  $\dot{Q}O_2$ -to- $\dot{V}O_2$  responses differ markedly for the two modes.

### **Competing interests**

The authors report no competing interests for this work.

### **Author contributions**

This work was completed at Kobe Design University, Japan. S.K., D.O., D.C.P., H.B.R., N.K. and T.J.B. contributed to the conception and design of the experiments. S.K., D.O. and N.K. were involved in data collection. All authors contributed to the analysis and interpretation of data. S.K. wrote the first draft of the article. All authors contributed to the critical revision of the paper and approved the final manuscript.

## **Funding**

Support for this study was provided by The Japan Society for the Promotion of Science, the Ministry of Education, Science and Culture of Japan (Grant-in-Aid 26560362 and 24247046 to S.K.).

## **Acknowledgements**

The authors would like to thank the participants who volunteered to take part in the study.

## References

1. **Andersen P, Adams RP, Sjogaard G, Thorboe A, and Saltin B.** Dynamic knee extension as model for study of isolated exercising muscle in humans. *J Appl Physiol* 59: 1647-1653, 1985.
2. **Barstow TJ.** CORP: Understanding near infrared spectroscopy (NIRS) and its application to skeletal muscle research. *J Appl Physiol* (Mar 7, 2019). doi:10.1152/jappphysiol.00166.2018.
3. **Beaver WL, Lamarra N, and Wasserman K.** Breath-by-breath measurement of true alveolar gas exchange. *J Appl Physiol Respir Environ Exerc Physiol* 51: 1662-1675, 1981.
4. **Bowen TS, Rossiter HB, Benson AP, Amano T, Kondo N, Kowalchuk JM, and Koga S.** Slowed oxygen uptake kinetics in hypoxia correlate with the transient peak and reduced spatial distribution of absolute skeletal muscle deoxygenation. *Exp Physiol* 98: 1585-1596, 2013.
5. **Brønstad E, Rognum O, Tjonna AE, Dedichen HH, Kirkeby-Garstad I, Haberg AK, Ingul CB, Wisloff U, and Steinshamn S.** High-intensity knee extensor training restores skeletal muscle function in COPD patients. *Eur Respir J* 40: 1130-1136, 2012.
6. **Chin LM, Kowalchuk JM, Barstow TJ, Kondo N, Amano T, Shiojiri T, and Koga S.** The relationship between muscle deoxygenation and activation in different muscles of the quadriceps during cycle ramp exercise. *J Appl Physiol* 111: 1259-1265, 2011.
7. **Cleland SM, Murias JM, Kowalchuk JM, and Paterson DH.** Effects of prior heavy-intensity exercise on oxygen uptake and muscle deoxygenation kinetics of a subsequent heavy-intensity cycling and knee-extension exercise. *Appl Physiol Nutr Metab* 37: 138-148, 2012.
8. **Damon DH, and Duling BR.** Are physiological changes in capillary tube hematocrit related to alterations in capillary perfusion heterogeneity? *Int J Microcirc Clin Exp* 6: 309-319, 1987.
9. **Davis ML, and Barstow TJ.** Estimated contribution of hemoglobin and myoglobin to near infrared spectroscopy. *Respir Physiol Neurobiol* 186: 180-187, 2013.
10. **DeLorey DS, Kowalchuk JM, and Paterson DH.** Relationship between pulmonary O<sub>2</sub> uptake kinetics and muscle deoxygenation during moderate-intensity exercise. *J Appl Physiol* 95: 113-120, 2003.
11. **Endo M, Okada Y, Rossiter HB, Ooue A, Miura A, Koga S, and Fukuba Y.**

- Kinetics of pulmonary  $\text{VO}_2$  and femoral artery blood flow and their relationship during repeated bouts of heavy exercise. *Eur J Appl Physiol* 95: 418-430, 2005.
12. **Esposito F, Reese V, Shabetai R, Wagner PD, and Richardson RS.** Isolated quadriceps training increases maximal exercise capacity in chronic heart failure: the role of skeletal muscle convective and diffusive oxygen transport. *J Am Coll Cardiol* 58: 1353-1362, 2011.
  13. **Federspiel WJ, and Popel AS.** A theoretical analysis of the effect of the particulate nature of blood on oxygen release in capillaries. *Microvasc Res* 32: 164-189, 1986.
  14. **Ferreira LF, Townsend DK, Lutjemeier BJ, and Barstow TJ.** Muscle capillary blood flow kinetics estimated from pulmonary  $\text{O}_2$  uptake and near-infrared spectroscopy. *J Appl Physiol* 98: 1820-1828, 2005.
  15. **Fukuba Y, Ohe Y, Miura A, Kitano A, Endo M, Sato H, Miyachi M, Koga S, and Fukuda O.** Dissociation between the time courses of femoral artery blood flow and pulmonary  $\text{VO}_2$  during repeated bouts of heavy knee extension exercise in humans. *Exp Physiol* 89: 243-253, 2004.
  16. **Fukuoka Y, Poole DC, Barstow TJ, Kondo N, Nishiwaki M, Okushima D, and Koga S.** Reduction of  $\text{VO}_2$  slow component by priming exercise: novel mechanistic insights from time-resolved near-infrared spectroscopy. *Physiol Rep* 3: e12432, 2015.
  17. **Grassi B.** Skeletal muscle  $\text{VO}_2$  on-kinetics: set by  $\text{O}_2$  delivery or by  $\text{O}_2$  utilization? New insights into an old issue. *Med Sci Sports Exerc* 32: 108-116, 2000.
  18. **Grassi B, Pogliaghi S, Rampichini S, Quaresima V, Ferrari M, Marconi C, and Cerretelli P.** Muscle oxygenation and pulmonary gas exchange kinetics during cycling exercise on-transitions in humans. *J Appl Physiol* 95: 149-158, 2003.
  19. **Harper AJ, Ferreira LF, Lutjemeier BJ, Townsend DK, and Barstow TJ.** Human femoral artery and estimated muscle capillary blood flow kinetics following the onset of exercise. *Exp Physiol* 91: 661-671, 2006.
  20. **Heinonen I, Koga S, Kalliokoski KK, Musch TI, and Poole DC.** Heterogeneity of Muscle Blood Flow and Metabolism: Influence of Exercise, Aging, and Disease States. *Exerc Sport Sci Rev* 43: 117-124, 2015.
  21. **Iannetta D, Okushima D, Inglis EC, Kondo N, Murias JM, and Koga S.** Blood flow occlusion-related  $\text{O}_2$  extraction "reserve" is present in different muscles of the quadriceps but greater in deeper regions after ramp-incremental test. *J Appl*

- Physiol 125: 313-319, 2018.
22. **Jones AM, Berger NJ, Wilkerson DP, and Roberts CL.** Effects of "priming" exercise on pulmonary O<sub>2</sub> uptake and muscle deoxygenation kinetics during heavy-intensity cycle exercise in the supine and upright positions. *J Appl Physiol* 101: 1432-1441, 2006.
  23. **Kindig CA, Richardson TE, and Poole DC.** Skeletal muscle capillary hemodynamics from rest to contractions: implications for oxygen transfer. *J Appl Physiol* 92: 2513-2520, 2002.
  24. **Klitzman B, and Duling BR.** Microvascular hematocrit and red cell flow in resting and contracting striated muscle. *Am J Physiol* 237: H481-490, 1979.
  25. **Knight DR, Schaffartzik W, Poole DC, Hogan MC, Bebout DE, and Wagner PD.** Effects of hyperoxia on maximal leg O<sub>2</sub> supply and utilization in men. *J Appl Physiol* 75: 2586-2594, 1993.
  26. **Koga S, Barstow TJ, Okushima D, Rossiter HB, Kondo N, Ohmae E, and Poole DC.** Validation of a high-power, time-resolved, near-infrared spectroscopy system for measurement of superficial and deep muscle deoxygenation during exercise. *J Appl Physiol* 118: 1435-1442, 2015.
  27. **Koga S, Barstow TJ, Shiojiri T, Takaishi T, Fukuba Y, Kondo N, Shibasaki M, and Poole DC.** Effect of muscle mass on Vo<sub>2</sub> kinetics at the onset of work. *J Appl Physiol* 90: 461-468, 2001.
  28. **Koga S, Kano Y, Barstow TJ, Ferreira LF, Ohmae E, Sudo M, and Poole DC.** Kinetics of muscle deoxygenation and microvascular PO<sub>2</sub> during contractions in rat: comparison of optical spectroscopy and phosphorescence-quenching techniques. *J Appl Physiol* 112: 26-32, 2012.
  29. **Koga S, Okushima D, Barstow TJ, Rossiter HB, Kondo N, and Poole DC.** Near-infrared spectroscopy of superficial and deep rectus femoris reveals markedly different exercise response to superficial vastus lateralis. *Physiol Rep* 5: e13402, 2017.
  30. **Koga S, Poole DC, Ferreira LF, Whipp BJ, Kondo N, Saitoh T, Ohmae E, and Barstow TJ.** Spatial heterogeneity of quadriceps muscle deoxygenation kinetics during cycle exercise. *J Appl Physiol* 103: 2049-2056, 2007.
  31. **Koga S, Poole DC, Fukuoka Y, Ferreira LF, Kondo N, Ohmae E, and Barstow TJ.** Methodological validation of the dynamic heterogeneity of muscle deoxygenation within the quadriceps during cycle exercise. *Am J Physiol Regul Integr Comp Physiol* 301: R534-541, 2011.
  32. **Koga S, Poole DC, Shiojiri T, Kondo N, Fukuba Y, Miura A, and Barstow TJ.**

- Comparison of oxygen uptake kinetics during knee extension and cycle exercise. *Am J Physiol Regul Integr Comp Physiol* 288: R212-220, 2005.
33. **Koga S, Rossiter HB, Heinonen I, Musch TI, and Poole DC.** Dynamic heterogeneity of exercising muscle blood flow and O<sub>2</sub> utilization. *Med Sci Sports Exerc* 46: 860-876, 2014.
  34. **Krustrup P, Soderlund K, Mohr M, Gonzalez-Alonso J, and Bangsbo J.** Recruitment of fibre types and quadriceps muscle portions during repeated, intense knee-extensor exercise in humans. *Pflugers Arch* 449: 56-65, 2004.
  35. **Ma S, Rossiter HB, Barstow TJ, Casaburi R, and Porszasz J.** Clarifying the equation for modeling of VO<sub>2</sub> kinetics above the lactate threshold. *J Appl Physiol* 109: 1283-1284, 2010.
  36. **MacDonald MJ, Shoemaker JK, Tschakovsky ME, and Hughson RL.** Alveolar oxygen uptake and femoral artery blood flow dynamics in upright and supine leg exercise in humans. *J Appl Physiol* 85: 1622-1628, 1998.
  37. **Malek MH, Coburn JW, and Tedjasaputra V.** Comparison of electromyographic responses for the superficial quadriceps muscles: cycle versus knee-extensor ergometry. *Muscle Nerve* 39: 810-818, 2009.
  38. **Murias JM, Spencer MD, and Paterson DH.** The critical role of O<sub>2</sub> provision in the dynamic adjustment of oxidative phosphorylation. *Exerc Sport Sci Rev* 42: 4-11, 2014.
  39. **Ohmae E, Nishio S, Oda M, Suzuki H, Suzuki T, Ohashi K, Koga S, Yamashita Y, and Watanabe H.** Sensitivity correction for the influence of the fat layer on muscle oxygenation and estimation of fat thickness by time-resolved spectroscopy. *J Biomed Opt* 19: 067005, 2014.
  40. **Okushima D, Poole DC, Barstow TJ, Rossiter HB, Kondo N, Bowen TS, Amano T, and Koga S.** Greater VO<sub>2peak</sub> is correlated with greater skeletal muscle deoxygenation amplitude and hemoglobin concentration within individual muscles during ramp-incremental cycle exercise. *Physiol Rep* 4: e13065, 2016.
  41. **Okushima D, Poole DC, Rossiter HB, Barstow TJ, Kondo N, Ohmae E, and Koga S.** Muscle deoxygenation in the quadriceps during ramp incremental cycling: Deep vs. superficial heterogeneity. *J Appl Physiol* 119: 1313-1319, 2015.
  42. **Poole DC, Copp SW, Ferguson SK, and Musch TI.** Skeletal muscle capillary function: contemporary observations and novel hypotheses. *Exp Physiol* 98: 1645-1658, 2013.
  43. **Poole DC, and Jones AM.** Oxygen uptake kinetics. *Compr Physiol* 2: 933-996, 2012.

44. **Poole DC, Musch TI, and Kindig CA.** In vivo microvascular structural and functional consequences of muscle length changes. *Am J Physiol* 272: H2107-2114, 1997.
45. **Poole DC, Richardson RS, Haykowsky MJ, Hirai DM, and Musch TI.** Exercise limitations in heart failure with reduced and preserved ejection fraction. *J Appl Physiol* 124: 208-224, 2018.
46. **Richardson RS, Frank LR, and Haseler LJ.** Dynamic knee-extensor and cycle exercise: functional MRI of muscular activity. *Int J Sports Med* 19: 182-187, 1998.
47. **Richardson RS, Knight DR, Poole DC, Kurdak SS, Hogan MC, Grassi B, and Wagner PD.** Determinants of maximal exercise  $\text{VO}_2$  during single leg knee-extensor exercise in humans. *Am J Physiol* 268: H1453-1461, 1995.
48. **Richardson RS, Poole DC, Knight DR, Kurdak SS, Hogan MC, Grassi B, Johnson EC, Kendrick KF, Erickson BK, and Wagner PD.** High muscle blood flow in man: is maximal  $\text{O}_2$  extraction compromised? *J Appl Physiol* 75: 1911-1916, 1993.
49. **Rossiter HB, Ward SA, Kowalchuk JM, Howe FA, Griffiths JR, and Whipp BJ.** Dynamic asymmetry of phosphocreatine concentration and  $\text{O}_2$  uptake between the on- and off-transients of moderate- and high-intensity exercise in humans. *J Physiol* 541: 991-1002, 2002.
50. **Saitoh T, Ferreira LF, Barstow TJ, Poole DC, Ooue A, Kondo N, and Koga S.** Effects of prior heavy exercise on heterogeneity of muscle deoxygenation kinetics during subsequent heavy exercise. *Am J Physiol Regul Integr Comp Physiol* 297: R615-621, 2009.
51. **Salvadeo D, Lazzar S, Marzorati M, Porcelli S, Rejc E, Simunic B, Pisot R, di Prampero PE, and Grassi B.** Functional impairment of skeletal muscle oxidative metabolism during knee extension exercise after bed rest. *J Appl Physiol* 111: 1719-1726, 2011.
52. **Shoemaker JK, Hodge L, and Hughson RL.** Cardiorespiratory kinetics and femoral artery blood velocity during dynamic knee extension exercise. *J Appl Physiol* 77: 2625-2632, 1994.
53. **Vogiatzis I, Habazettl H, Louvaris Z, Andrianopoulos V, Wagner H, Zakyntinos S, and Wagner PD.** A method for assessing heterogeneity of blood flow and metabolism in exercising normal human muscle by near-infrared spectroscopy. *J Appl Physiol* 118: 783-793, 2015.
54. **Volianitis S, and Secher NH.** Cardiovascular control during whole body exercise. *J Appl Physiol* 121: 376-390, 2016.

55. **Whipp BJ, Rossiter HB, and Ward SA.** Exertional oxygen uptake kinetics: a stamen of stamina? *Biochem Soc Trans* 30: 237-247, 2002.

Table 1. Pulmonary O<sub>2</sub> uptake kinetics during cycling and knee extension exercise

	Cycling		Knee extension	
Work rate (W)	189 ±	22	82 ±	10 *
Baseline (mL·min <sup>-1</sup> )	581 ±	67	580 ±	67
A' <sub>c</sub> (mL·min <sup>-1</sup> )	370 ±	109	215 ±	46 *
TD <sub>p</sub> (s)	22 ±	4	25 ±	9
τ <sub>p</sub> (s)	33 ±	13	41 ±	23
A' <sub>p</sub> (mL·min <sup>-1</sup> )	1662 ±	203	750 ±	136 *
G <sub>p</sub> (mL·min <sup>-1</sup> ·W <sup>-1</sup> )	9.9 ±	0.7	12.3 ±	1.9 *
TD <sub>s</sub> (s)	174 ±	55	167 ±	53
A' <sub>s</sub> (mL·min <sup>-1</sup> )	253 ±	183	167 ±	116
A' <sub>s</sub> /(A' <sub>p</sub> +A' <sub>s</sub> )	0.13 ±	0.09	0.17 ±	0.09
ΔV̇O <sub>2 6-3</sub> (mL·min <sup>-1</sup> )	184 ±	49	124 ±	71
ΔEE V̇O <sub>2</sub> (mL·min <sup>-1</sup> )	1912 ±	192	912 ±	193 *

Values are means ± SD (n = 8).

\*, P < 0.05 for paired t-test.

V̇O<sub>2</sub>, pulmonary O<sub>2</sub> uptake; A'<sub>c</sub>, amplitude of cardiodynamic component; TD<sub>p</sub>, time delay of primary component; τ<sub>p</sub>, time constant of primary component; A'<sub>p</sub>, amplitude of primary component; G<sub>p</sub>, the O<sub>2</sub> cost (gain) of the primary component V̇O<sub>2</sub>; TD<sub>s</sub>, time delay of slow component; A'<sub>s</sub>, amplitude of the slow component at end exercise; ΔV̇O<sub>2 6-3</sub>, the increment in V̇O<sub>2</sub> between the 3rd and 6th min of exercise; ΔEE V̇O<sub>2</sub>, end-exercise V̇O<sub>2</sub> above the baseline.

Table 2. Amplitude and kinetic characteristics of the deoxy[Hb+Mb] response among the superficial muscles following the onset of heavy exercise of cycling (CE) and knee extension (KE).

		Vastus lateralis		Rectus femoris		
		Distal (dVL-s)		Distal (dRF-s)		Proximal (pRF-s)
Baseline ( $\mu\text{M}$ )	CE	50.0	$\pm$ 4.3	53.5	$\pm$ 7.9	52.4 $\pm$ 6.0
	KE	55.8	$\pm$ 4.2 †	57.6	$\pm$ 5.3 †	61.8 $\pm$ 6.6 †
Amplitude ( $\mu\text{M}$ )	CE	40.4	$\pm$ 27.4	22.6	$\pm$ 11.0 a	19.7 $\pm$ 12.8 a
	KE	25.1	$\pm$ 14.2 †	25.6	$\pm$ 14.1	19.3 $\pm$ 11.5
Time delay (s)	CE	4	$\pm$ 1	7	$\pm$ 4	11 $\pm$ 8 a
	KE	8	$\pm$ 3	4	$\pm$ 3	4 $\pm$ 4 †
Time constant (s)	CE	15	$\pm$ 3	28	$\pm$ 15	40 $\pm$ 18 a
	KE	43	$\pm$ 16 †	24	$\pm$ 9 a	21 $\pm$ 9 a†
Mean response time (s)	CE	19	$\pm$ 4	35	$\pm$ 19	51 $\pm$ 23 a
	KE	51	$\pm$ 16 †	28	$\pm$ 11 a	25 $\pm$ 12 a†
$r^2$	CE	0.95	$\pm$ 0.05	0.86	$\pm$ 0.20	0.82 $\pm$ 0.23
	KE	0.92	$\pm$ 0.05	0.95	$\pm$ 0.03	0.90 $\pm$ 0.05

Values are means  $\pm$  SD (n = 8).

“a”, vs. distal site of vastus lateralis,  $P < 0.05$ . †, vs. cycling exercise,  $P < 0.05$ .

$r^2$ , Coefficient of determination

Table 3. Amplitudes of the deoxy[Hb+Mb] response in the superficial- and deep muscles following the onset of heavy exercise of CE and KE.

		Vastus lateralis				Rectus femoris			
		Distal (dVL-s)		Proximal (deep, pVL-d)		Distal (dRF-s)		Proximal (pRF-s)	
Baseline ( $\mu\text{M}$ )	CE	50.0	$\pm$ 4.3	48.7	$\pm$ 6.9	53.5	$\pm$ 7.9	52.4	$\pm$ 6.0
	KE	55.8	$\pm$ 4.2 †	59.2	$\pm$ 5.6 †	57.6	$\pm$ 5.3 †	61.8	$\pm$ 6.6 †
Amplitude at 3 min ( $\mu\text{M}$ )	CE	39.8	$\pm$ 25.6	25.5	$\pm$ 36.8	21.4	$\pm$ 10.1	19.4	$\pm$ 12.7
	KE	23.6	$\pm$ 13.6 †	18.8	$\pm$ 23.6 †	22.5	$\pm$ 14.5 †	17.3	$\pm$ 11.1 †
Amplitude at 6 min ( $\mu\text{M}$ )	CE	44.5	$\pm$ 25.3	27.4	$\pm$ 35.3	27.4	$\pm$ 14.1	23.8	$\pm$ 15.9 a
	KE	25.6	$\pm$ 11.2 †	19.6	$\pm$ 20.8 †	25.3	$\pm$ 14.2 †	18.7	$\pm$ 9.6 a†
$\Delta$ Amplitude <sub>6-3</sub> ( $\mu\text{M}$ )	CE	4.7	$\pm$ 4.4	1.9	$\pm$ 3.3	6.0	$\pm$ 5.1	4.5	$\pm$ 5.0
	KE	2.0	$\pm$ 4.0	0.9	$\pm$ 4.2	2.7	$\pm$ 2.2	1.4	$\pm$ 4.4
Relative amplitude of slow component	CE	0.12	$\pm$ 0.10	0.14	$\pm$ 0.97	0.23	$\pm$ 0.17	0.17	$\pm$ 0.15
	KE	0.05	$\pm$ 0.34	0.05	$\pm$ 0.86	0.13	$\pm$ 0.15	0.05	$\pm$ 0.30

Values are means  $\pm$  SD (n = 8).

“a”, vs. distal site of vastus lateralis,  $P < 0.05$ . †, vs. cycling exercise,  $P < 0.05$ .

Table 4. Amplitudes of the total[Hb+Mb] response in the superficial- and deep proximal VL muscles following the onset of heavy exercise of CE and KE.

		Vastus lateralis		Rectus femoris	
		Distal (dVL-s)	Proximal (deep, pVL-d)	Distal (dRF-s)	Proximal (pRF-s)
Baseline ( $\mu\text{M}$ )	CE	186.6 $\pm$ 11.6	192.9 $\pm$ 20.8	198.8 $\pm$ 12.5	197.8 $\pm$ 18.0
	KE	192.8 $\pm$ 12.4	196.8 $\pm$ 17.7	206.3 $\pm$ 8.2	202.0 $\pm$ 18.5
Amplitude at 3 min ( $\mu\text{M}$ )	CE	15.9 $\pm$ 6.9	-2.9 $\pm$ 6.6 a	6.1 $\pm$ 2.3 a	1.0 $\pm$ 9.7 a
	KE	21.1 $\pm$ 6.5 †	10.9 $\pm$ 12.9 a†	10.9 $\pm$ 5.6 a†	6.5 $\pm$ 3.5 a†
Amplitude at 6 min ( $\mu\text{M}$ )	CE	16.3 $\pm$ 7.5	-1.8 $\pm$ 10.0 a	12.2 $\pm$ 5.2 b	6.3 $\pm$ 11.9
	KE	23.0 $\pm$ 6.2	15.6 $\pm$ 15.0 †	12.1 $\pm$ 6.0	8.6 $\pm$ 6.6 a
$\Delta$ Amplitude <sub>6-3</sub> ( $\mu\text{M}$ )	CE	0.3 $\pm$ 4.0	1.1 $\pm$ 4.7	6.2 $\pm$ 3.6	5.3 $\pm$ 3.7
	KE	1.9 $\pm$ 7.6	4.7 $\pm$ 6.8	1.2 $\pm$ 2.0 †	2.1 $\pm$ 4.3

Values are means  $\pm$  SD (n = 8).

“a”, vs. distal site of vastus lateralis, P < 0.05. “b”, vs. proximal site of vastus lateralis, P < 0.05. †, vs. cycling exercise, P < 0.05.

## Figure Legends

Figure 1. Panel “a”; Group mean responses of pulmonary  $\dot{V}O_2$  following the onset of heavy-intensity cycling (CE, solid line) and knee extension exercise (KE, dotted line).

Panel “b”; Pulmonary  $\dot{V}O_2$  per power (gain) during CE and KE.

Figure 2. Group mean responses for muscle deoxy[Hb+Mb] from baseline to heavy exercise of CE (panel a) and KE (panel b). Open and gray circles show responses for distal (superficial) and proximal (deep) VL. Open and filled squares show responses for superficial sites of distal and proximal RF, respectively.

Figure 3. Comparison of relative increases between pulmonary  $\dot{V}O_2$  and muscle deoxy[Hb+Mb] responses from baseline to heavy exercise of CE (panel a) and KE (panel b). Open and gray circles show the group mean responses for deoxy[Hb+Mb] in superficial and deep VL, respectively. Thick solid line shows the group mean responses for pulmonary  $\dot{V}O_2$ .

Figure 4. Group mean responses of total[Hb+Mb] from baseline to heavy exercise for CE (panel a) and KE (panel b). Open and gray circles show responses for distal (superficial)

and proximal (deep) VL. Open and filled squares show responses for superficial sites of distal and proximal RF, respectively.

Figure 5. Group mean responses for point-by-data point root mean square error (RMSE) changes (i.e., inter-site heterogeneity across the quadriceps muscles) of muscle deoxy- (panel a) and total[Hb+Mb] (panel b) following the onset of heavy exercise. Open and filled triangles show the changes in KE and CE, respectively. \* shows the significant differences between KE and CE ( $P < 0.05$ ).

Figure 6. Group mean responses of muscle activity (iEMG) relative to MVC (% MVC) during the last 30 s immediately before the end of heavy-intensity exercise for CE and KE. # denotes the significant differences from both proximal and distal VL muscles ( $P < 0.05$ ).

Figure 7. Group mean amplitudes of deoxy- (panel a) and total[Hb+Mb] (panel b) normalized to iEMG (i.e.,  $\mu\text{M} \cdot \% \text{MVC}^{-1}$ ) during heavy-intensity exercise for CE and KE. \$ denotes the significant differences between KE and CE ( $P < 0.05$ ).

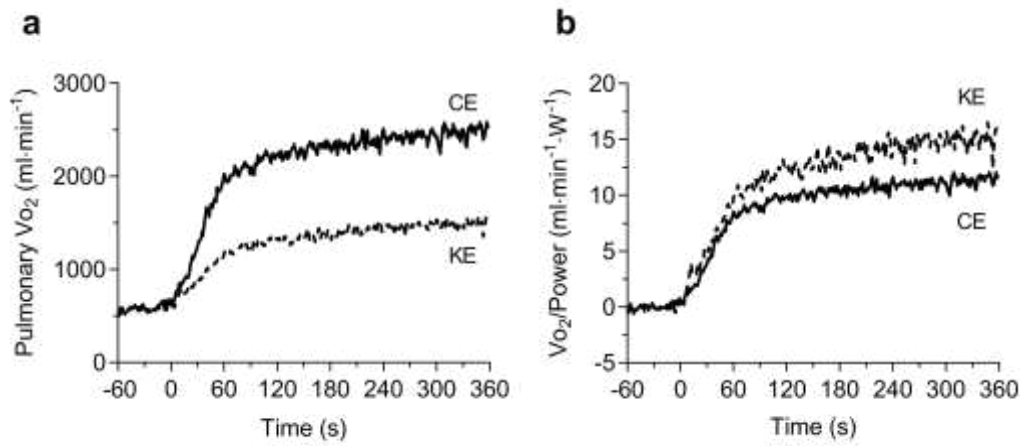


Figure 1.

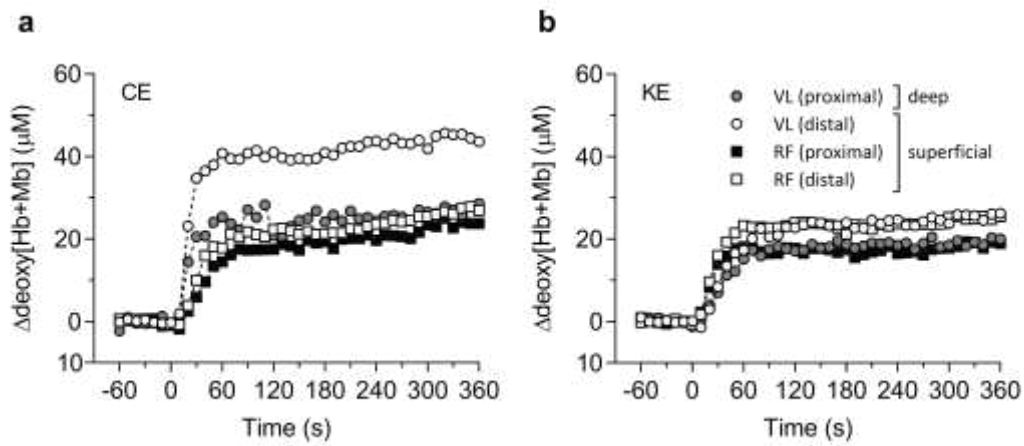


Figure 2.

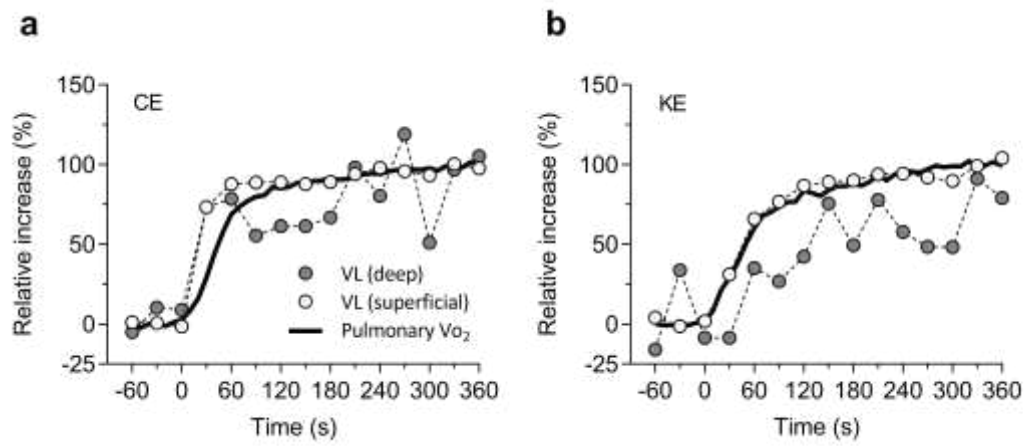


Figure 3.

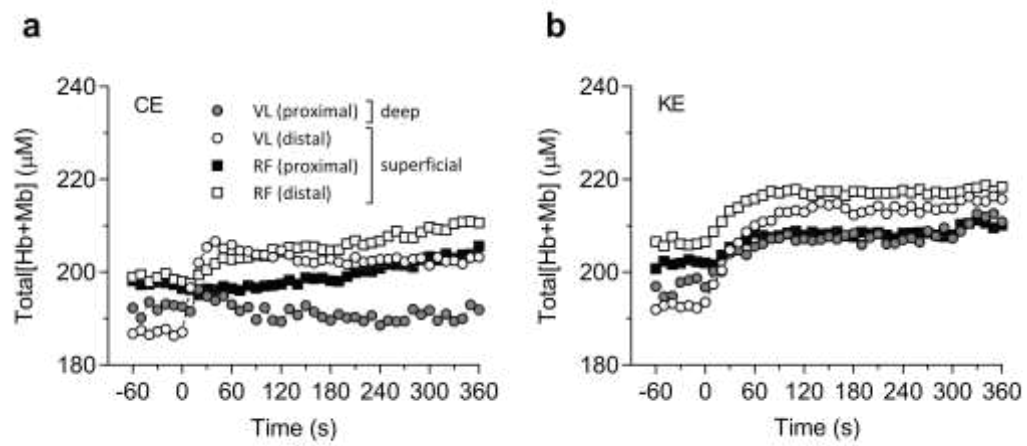


Figure 4.

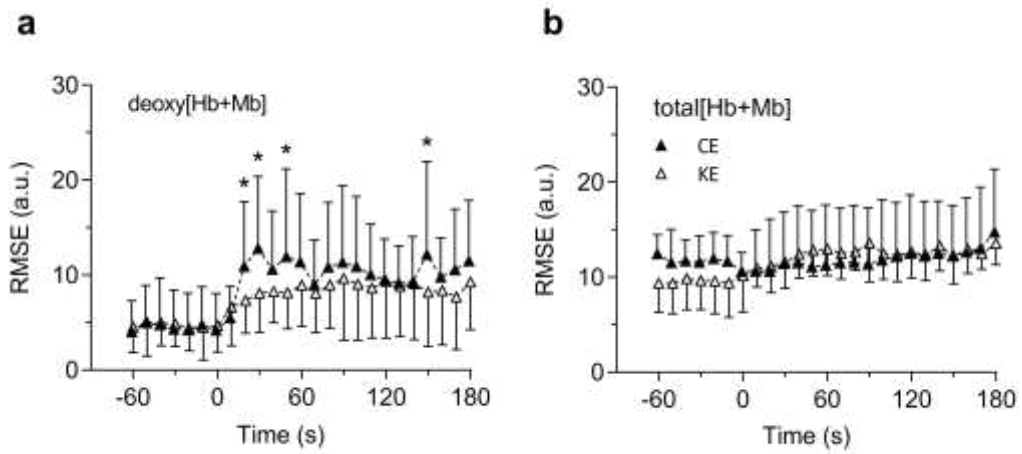


Figure 5.

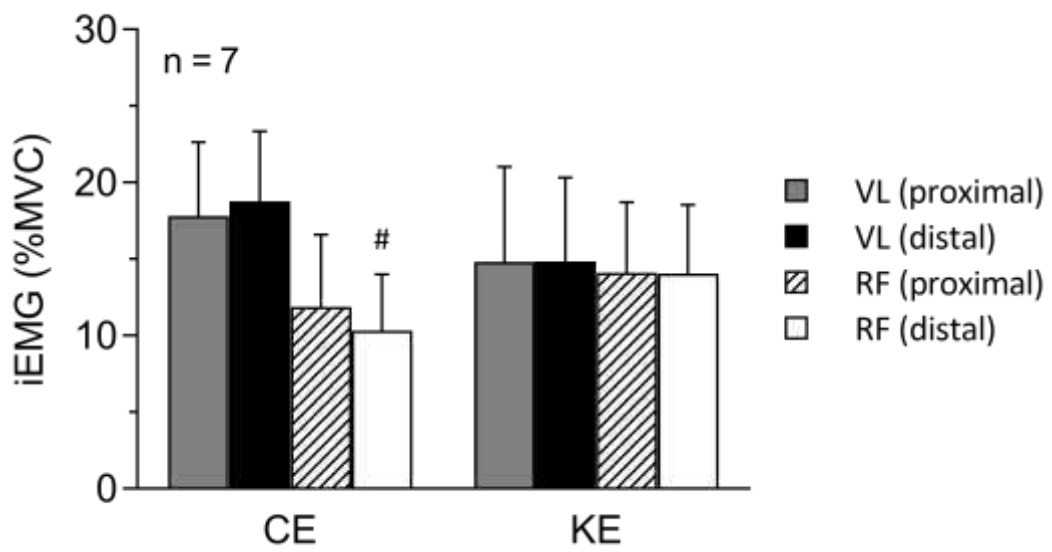


Figure 6.

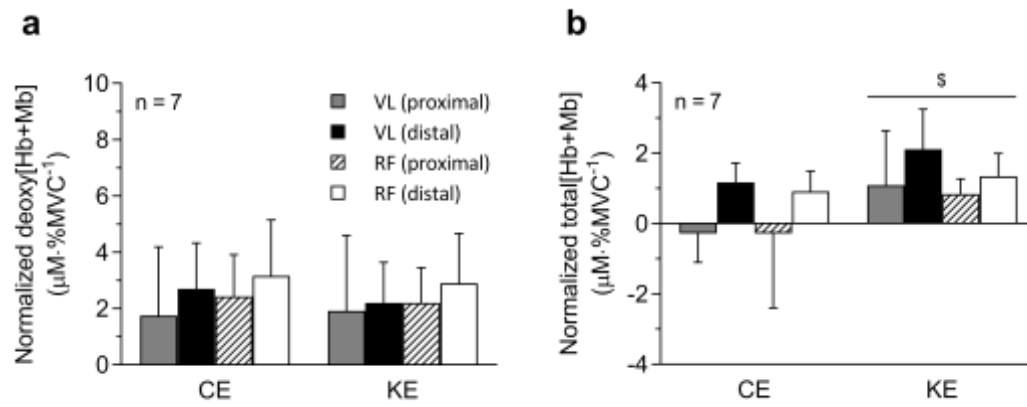


Figure 7.